CHAPTER 27

A ROBUST ALGORITHM FOR NONDESTRUCTIVE TESTING OF WELD SEAMS

Miguel A. Carrasco and Domingo Mery

Departamento de Ciencia de la Computación
Pontificia Universidad Católica de Chile.
Av. Vicuña Mackenna 4860 (143). Santiago de Chile
mlcarras@puc.cl; dmery@ing.puc.cl

The detection of welding flaws by means of nondestructive inspection methods remains open to the development of new algorithms and methods of inspection. One of the most widely used techniques is radiographic analysis, which requires interpretation by trained inspectors. Unfortunately, manual inspection is subject to various factors that can alter performance in the detection of the faults. An automated welding fault segmentation algorithm is presented using a set of digitized radiographic images. The result of the study has allowed the development of the following scheme: first, use the median filter to reduce noise; second, apply the bottom-hat filter to separate the hypothetical faults from the background; third, determine the segmented regions by binary thresholding; fourth, use the filters provided by morphological mathematics to eliminate over segmentation; and fifth, use the watershed transform to separate the internal regions. The results of the study have generated a general ROC curve on a set of 10 images with an area A_z=93.6%.

1. Introduction

Quality control of manufactured products has become one of the main objectives of production processes. For its evaluation several inspection and analysis techniques are available that can be applied during the manufacturing process, but all of them depend on the fulfillment of safety standards imposed by the manufacturer or by some regulatory standard. Although some manufacturers tolerate faulty products, for others products safety plays a critical role. Traditionally, quality control has been carried out manually by an inspector, because human inspection is flexible and adaptable to new situations that have not been considered, but this process itself has serious drawbacks such as i) Time

consuming: it takes a large amount of time and it is dependent on weariness and monotony at work; ii) Inconsistency: it depends on the inspector's capacity and experience for its analysis. These factors have led industry to gradually replace human inspection by automatic methods. One of the conventional forms of applying automatic inspection has been through machine vision systems. The objective is to determine automatically if the product fulfills a set of previous specifications using only visual information. This methodology is known as Automatic Visual Inspection (AVI), a name that encompasses a large set of analyses and algorithms that are divided into a series of processing stages that include image formation, preprocessing, segmentation, extraction of characteristics, and classification.

AVI has largely solved visual quality control, setting precise and objective control policies [1]. The main objective is to determine whether a product falls within or outside the range of acceptance in the manufacturing process. To that end it has to fulfill two basic conditions to improve product quality: efficiency and speed [2]. i) Efficiency means detecting the large number of defective products, and at the same time rejecting the smallest number of products in good condition. ii) Speed means that the production process is not affected by the time taken for the inspection, i.e. that production speed is maintained or increased. Current methods aim at decreasing the number of false positives and false negatives. Ideally these variables should be 0%, however this is difficult to achieve because it depends on the kind of product that is being analyzed. The decision to decrease some of these variables affects the performance of AVI quality control. Some of the effects of the adjustment can be: to detect 100% of products free from defects and reject a margin of products in good condition; or to accept a margin of defective products together with all the products in good condition.

Table 1. Examples of recent automatic visual inspection techniques

Textiles	Mamic *et al* (2000); Zhang, *et al* (2005)	[3, 4]
Welding	Liao (2003); Carrasco & Mery (2004)	[5, 6]
Bearings	Liang-Yu L. *et al* (2005)	[7]
Automobile doors and glass	Yun Koo Chung (1998)	[8]
Vehicle wheels	Mery *et al* (2002); Carrasco & Mery (2006)	[9, 10]
Aircratf turbines	Nguyen *et al* (1998)	[11]
Printed circuits	Park *et al* (2006)	[12]
Food	Pedreschi *et al* (2004)	[13]
Glass bottles	Mery & Medina (2004); Shafait, *et al* (2004)	[14, 15]
Wood	Lihari & Obac (2005)	[16]

In general, the applications of AVI are found in different areas of industry, such as detection of faults in printed circuits, welds, glass, textiles, food, aluminum wheels, bearings, aircraft turbines, etc. Therefore, every inspection is directly related to the kind of material that it is desired to analyze (see Table 1). A method designed for recognizing faults in one material may not be applicable to another [2].

One of the most important quality control areas for determining faults in welded structures has traditionally been done with radiographs, and in recent years with time-of-flight diffraction (TOFD) ultrasound techniques. Radiography allows the inspection of the quality of structures made from metals or other materials by making X-rays or γ-rays go through them. The faults are shown by the different light intensities generated by capturing the energy transmitted by the radiation on the radiographic images [17]. Ultrasound techniques use high frequency sound waves to detect the faults. TOFD is based on measuring the time and amplitude taken by the wave to travel from the emitter to a receptor along the weld. The faults are revealed by an alteration of the waves if they are found between the surface and the background of the material [18]. The above techniques have the advantage that the analyzed material is not destroyed during the inspection process, but both share the same problems of manual quality control, because the quality of the inspection is largely dependent on the quality and training of the inspector.

The field that covers nondestructive tests is known as NDT, and it involves various inspection techniques whose objective is to ensure that the design and operation requirements are safe and reliable. For that purpose different inspection techniques have been developed [19], the most common of which are the methods of radiographic analysis and of ultrasound described above. According to Moura *et al* [20], ultrasound methods have comparative advantages over radiographic methods as they avoid the effects of ionizing radiation on the operators and the use of radiographic films or plates which in some cases degrade the quality of the images [21]. However, classification of defects through ultrasound methods is often questioned because it is highly subjective, since the analysis and identification depend exclusively on the experience and knowledge of the operator. On the other hand, radiographic methods are the most widely used as inspection methods of welds in NDT. Their development and research continue being applied in industry and in science, leading to technical and/or economic advantages [22].

According to Liao [5], most radiographic inspection procedures have three parts: segmentation of the weld joints on the background,[a] segmentation of the flaws on the weld joints, and classification of the flaws. Our research begins with the second step, i.e. the position of the weld joint is known. Therefore, our approach consists in segmenting the largest number of flaws in the welds. Segmentation is commonly considered one of the most complex tasks in image processing [24]. Research in this field is extensive, but it is specific to the material that is being analyzed. In this research, different strategies and methods have been evaluated, oriented at the detection of faults in images of welds supplied by BAM[b].

This chapter is organized as follows: Section 2 presents the state of the art in flaw detection in welds; Section 3 presents the segmentation methods and the solution scheme developed in this study; Section 4 presents the results obtained; and Section 5 presents our conclusions. An extended version of this article may be found in [25].

2. State of the Art

There are structures that use welds for critical functions, such as high pressure equipment, chemical compounds, etc, where any kind of flaw can trigger catastrophic consequences. The conventional forms for detecting welding flaws are by means of visual inspection of radiographic images. The images are generated by using X-rays and γ-rays which penetrate the material generating a radiological image on a photographic plate. Flaws are detected due to variations in the density of the material (see Fig. 1). Nonetheless, manual interpretation of flaws can generate subjective and imprecise results which require a great deal of time and are inconsistent in that they depend on an inspector for their analysis [5].

Due to the problems associated with manual detection, there is currently a great deal of work and research on non-destructive testing (NDT) methods for detecting welding defects. The objective is to develop an automated method for the detection of defects that is precise and objective. Some of the most important achievements in this area are presented below.

[a] An application to determine the position and orientation of welded joints is available in [23]

[b] The images for this research are part of a set of radiographic images of welds generated by the Federal Institute for Materials Research and Testing, Berlin (BAM).

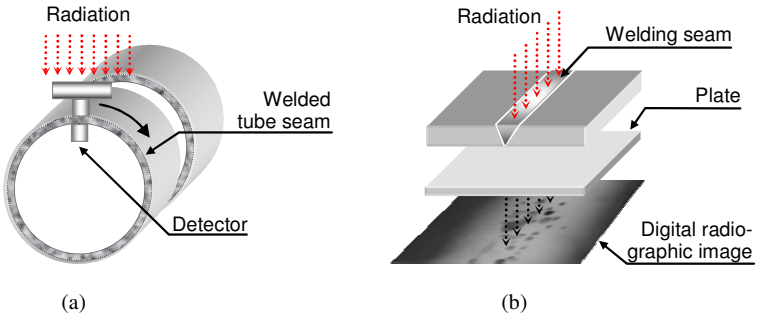

Figure 1. (a) Flaw detection scheme through radiation of weld. (b) Radiation over material flaw captured on a radiographic plate.

Gayer *et al* [26] proposed a method that can be summarized as having two steps: i) A quick search for potential defects in the X-ray image: Assuming that the defects will be smaller than the regular structure of the test piece, potential defects are classified as those regions of the image where higher frequencies are significant. The spectrum of the X-ray image is determined with the help of a fast Fourier transformation, which is calculated either row by row or column by column in small 32×32 windows. When the sum of the higher frequencies of a window is greater than a given threshold value, the entire window is marked as potentially defective. Another possibility is suggested by the authors as part of this task: A window is selected as potentially defective when the sum of the first derivative of the rows and columns of a window is large enough. ii) Identification and location of the true defect: Because of the time-consuming nature of this step, only those regions which were previously classified as being potentially defective were studied here. Two algorithms were developed here as well. The first leads to a matching between the potential defect and typical defects, which are stored in a library as templates. Whenever a large resemblance between the potential defect and a template is found, the potential defect is classified as a true defect. The second algorithm estimates a defect-free X-ray image of the test piece by modeling every line of an interpolated spline function without special consideration for the potentially defective region. Following this, the original and the defect-free images are compared. True defects are identified when large differences occur compared to the original input image.

Lawson and Parker [27] proposed that artificial neural networks (ANN) be used for the automated detection of defects in X-ray images. The method generates a binary image from the test image where each pixel is either 0 when a regular structure feature of the piece exists or 1 when a defect is detected. This entails the supervised learning of a multi-layer perceptron network (MLP) where

an attempt is made to obtain detection from training data. A back propagation algorithm is used for the assignment of weights within the MLP. The authors use one or two hidden layers in the network topography of the ANN, where the input signal corresponds to a window of $m \times m$ grey values in the X-ray image. The output signal is the pixel at the image centre in the binary image. Since the threshold value function for the neurons is sigmoidal in this method, a threshold is used to obtain a binary output signal. The desired detection in the training data was obtained with a segmenting procedure based on an adaptive threshold. During the experiments with five X-ray images, the authors showed that detection using ANN is superior to the segmenting method using adapted thresholds.

Sofia and Reduane [28] proposed a method for automated recognition of welding defects. The detection follows a pattern recognition methodology: i) Segmentation: regions of pixels are found and isolated from the rest of the X-ray image using a watershed algorithm and morphological operations (erosion and dilation). ii) Feature extraction: the regions are measured and shape characteristics (diameter variation and main direction of inertia based on invariant moments) are quantified. iii) Classification: the extracted features of each region are analyzed and classified using a k-nearest neighbor classifier. According to the authors, the method is robust and achieves a good detection rate.

Silva *et al* [29] proposed another welding defect classification method. In a first step, called image pre-processing, the quality of the X-ray image is improved using a median filter and a contrast enhancement technique. The defect detection follows the pattern recognition scheme mentioned above: i) Potential defects are segmented in the X-ray image. ii) Geometric and grey value features (contrast (C), position (P), aspect ratio (a), width-area ratio (e/A), length-area ratio (L/A) and roundness(R)) are extracted. The correlation between features and each defect class considered (slag inclusion, porosity, lack of penetration and undercutting) was evaluated by analyzing the linear correlation coefficient. iii) The most relevant features were used as input data on a hierarchic linear classifier [29]. In order to achieve a higher degree of reliability of the results, radiographic standards from the International Institute of Welding were used, with 86 films containing the main defect classes. The experimental results show that features P and e/A are able to classify the undercutting and lack of penetration classes. Nevertheless, the six mentioned features are required to obtain high performance by classifying the porosity and inclusion defects.

Liao and Li [30] proposed a detection approach based on curve fitting. The key idea of this work is to simulate a 2D background for a normal welding bead

characterized by low spatial frequencies in comparison with the high spatial frequencies of defect images. Thus, a 2D background is estimated by fitting each vertical line of the weld to a polynomial function, and the obtained image is subtracted from the original image. The defects are detected where the difference is considerable. Wang & Liao [31] and Liao [5] proposed a fuzzy k-nearest neighbor, multi-layer perceptron neural network and a fuzzy expert system for the classification of welding defect types. The features used for the classification are distance from centre, circularity, compactness, major axis, width and length, elongation, Heywood diameter, and average intensity and standard deviation of intensity. Finally the (K-NN) and the (MLP) methods are used for classification. The results indicate that the (MLP) method is superior to the (K-NN) method, classifying 92.39% and 91.57% respectively.

Mery and Berti [32] presented a new methodology based on texture analysis. Texture is one of the most important characteristics in pattern recognition, but it has seen limited use in the analysis of digital images in NDT. The referenced study examines the analysis of two types of texture features: those based on the occurrence matrix, and those based on the Gabor function. The proposed approximation uses the following methodology: i) Segmentation: the LoG edge detector is used. ii) Extraction of characteristics: the features of potential defects are extracted. iii) Classification: the most relevant features are used as input data for a statistical classifier. The best results have been achieved with a polynomial classifier, with 91% defect detection, and 8% false alarm rate.

Li *et al* [33] proposed the development of an adaptive segmentation algorithm through genetic algorithms (GA) [34]. One of the major problems of segmentation is the determination of an appropriate threshold value that allows the separation of the relevant objects from the background. One of the most widely used methods is that of Otsu [35], because it determines an optimum threshold value for two classes. Unfortunately, the weld images contain more than two classes due to the surface of the object, light interference, etc. According to Li *et al*, the solution consists in generalizing Otsu's method as a multiple class problem that can be tackled through a genetic algorithm. The results indicate that the designed method is adaptive and efficient at generating a segmentation in welded joints.

Wang & Wong [36] presented a welding flaw segmentation method by means of the Fuzzy C-Means algorithm. The method consists of three steps: First, the top-hat and bottom-hat filters are applied. These filters extract the light from the objects generating low changes over the background of the image. The defects can thus be stressed and the background regions can be eliminated. Second, apply an adaptive wavelet thresholding filter (proposed by Donoso [37]). The purpose

of this filter is to eliminate the noise present in the signal while preserving the characteristics of the signal. According to Chang *et al* [38], this filter retains the sharpness of the edges of the defects better than the median filter. Third, use a fuzzy c-means (FCM) clustering algorithm. The clustering allows the assignment of a class depending on the degree of similarity that there is in the patterns that make it up [39]. One of the advantages of using this technique is that it allows the use of any number of characteristics and assign them to any number of classes, in addition to being applicable to instances in an unsupervised way. According to Wang & Wong, this technique has a more efficient performance compared to the method of Otsu, so the fuzzy c-means algorithm can detect a greater number of flaws in the welds.

Movafeghi *et al* [40] proposed improving the quality of the digitized radiographic images to intensify the location and recognition of the flaws. The research proposes the independent use of three techniques, two in the space domain, filters through morphologic mathematics and pseudo-color, and one in frequency, the wavelet filter. The morphologic mathematics technique consists in first applying a median filter to reduce the noise level and retain the edges, and then using a bottom-hat and top-hat filter operation. The pseudo-color technique converts the image from grey levels to a new color image using color mapping. The objective is to improve the visualization of the flaws. The wavelets technique makes it possible to decompose the image into subcomponents in the frequency and time domains. The idea is to select only those coefficients that have more information and eliminate the high frequency coefficients, which contain most of the noise. Then the reverse transformation is carried out and the image is reconstructed. This methodology has been used in radiological applications in mamography [41]. The results indicate that the morphologic mathematics technique has the best performance, with S_n=90% and 1-S_p=0%. According to the authors, the application of wavelets has greater complexity and must have supervised training.

Kleber *et al* [23] developed a methodology for extracting and limiting the weld joints in radiographic images. In various researches, analysis of the welds starts with a segmentation between the weld regions, discarding the background, but this requires a previous knowledge because it is necessary to determine the location, width, length and angle of the weld. Furthermore, the problem is increased due to markers and indicators that are inserted in the radiographic image. The methodology proposed by Kleber *et al.* uses a genetic algorithm (GA) [34] to locate the position of the welds using a model stored previously in the system. The objective is for the GA to determine the best position that matches

the stored model. The results have a 94.4% yield for detecting weld joints, either in different location, width, length and angle.

The literature reviewed includes a large number and variety of methodologies for the detection of welding defects, such as interpolating the image's background curves, neuronal networks, geometric characteristics, application of mathematical morphology and the watershed algorithm, texture analysis, etc. Research in this area continues largely because there are, as yet, no satisfactory results that allow the detection of all flaws without false alarms. Moreover, it is not possible to determine which of the research directions will improve the overall results, because each of them has room for improvement. The research presented in this paper is justified as it develops a new segmentation method which improves the process of automated detection of welding defects. Moreover, it also involves the development of a methodology that brings together some of the best characteristics of the reviewed studies, such as application of a median filter [29], comparison between a real image and a defect-free image [30], the use of mathematical morphology, and the watershed algorithm [28].

3. Steps of the Proposed Segmentation Algorithm

Segmentation consists in partitioning the image into disjoint regions, where each region is homogenous with respect to a given property, such as texture, grey level, type of color, etc., with the purpose of separating regions of interest for their later recognition [24]. Thus, the segmentation problem can be approached with different methods, which generally can be categorized into three types of techniques: those oriented to the detection of edges, pixel detection, and region detection [42].

In our study the edge detection was done first using gradient approaches. The Roberts, Prewitt, Sobel, and Laplace of Gaussian [42] filters belong to this category. These calculate the gradient, and according to some threshold level determine if a possible edge exists. Subsequently the Canny filter [43] was reviewed. This filter uses a combination of techniques, such as the Gaussian filter, for the elimination of noise, as well as making use of directional gradients, thus allowing the selection of only those edges that are found within the specified threshold. In pixel detection we have thresholding [42], which is a widespread technique as it allows the conversions of an image in grey scale to a binary image in such a way as to separate background objects according to a specified threshold. The watershed transform [44] is used in region detection. This technique makes use of morphological mathematics and allows the generation of regions based on cavity filling, simulating a valley filling with water; as the water

level rises, adjacent regions start forming unions. We also studied the distance transform [45] and the manner in which it can improve segmentation quality by using the watershed transform. In this case segmentation is used with the purpose of separating known regions from "hypothetical defects". These regions are made of true defects as well as false alarms, and it is the task of the classifier to correctly separate these two groups according to a set of geometric properties such as area, perimeter, invariant moments, etc., which are analyzed in the characteristic extraction process [9].

The proposed segmentation process uses a combination of digital processing techniques which have been selected on the basis of experimental tests and analyses, the development of which is presented in Fig. 2. Each stage has been analyzed independently and globally, allowing the study of different variations and strategies.

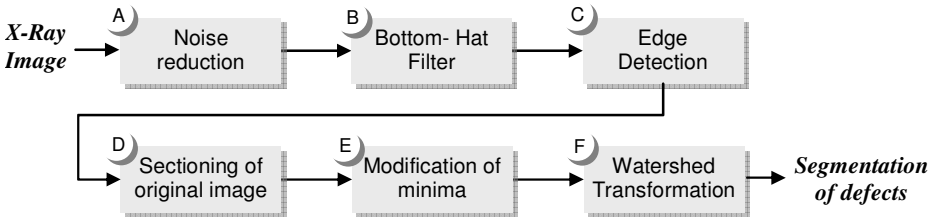

Figure 2. Proposed segmentation process for the detection of flaws in radiographic images.

A) Noise Reduction: The purpose of this phase is to attenuate the largest amount of noise in order to improve the segmentation process. There are different types of noise in an image, such as Gaussian, impulsive, frequential and multiplicative noise [42], and for that reason reduction is difficult, especially in radiographic images. Even though there is a large number of noise reduction filters, in this work we analyzed three techniques: the average, the Gaussian, and the median filters. Each filter has the purpose of attenuating in the best way some kind of noise, and they are therefore evaluated specifically in the BAM images. According to the experimental tests carried out, the median filter has at least two advantages with respect to the average and Gaussian filters: i) it is a more robust indicator, because an unrepresentative pixel does not introduce its value in the result, and ii) it does not generate new pixels when working on the edges. The median filter is therefore much better for preserving the edges clearly. Other research has shown the advantage of using the median filter. Such is the case of flaw detection in glass bottles [14].

B) Bottom-Hat Filter: The bottom-hat filter is used to highlight structures with hypothetical flaws and separate them from the background [46]. This process consists of two stages: i) First, use the morphologic lock operator on the original image, for which it is required that the size of the nucleus applied to the lock must allow the elimination of most hypothetical flaws, and as a consequence a background similar to that of the original image is generated, but without flaws. ii) Second, use the subtraction operator between the original image and the modified image from the first stage. As a result, the smaller structures, which in general are flaws, are revealed because of their separation from the background (Fig. 3).

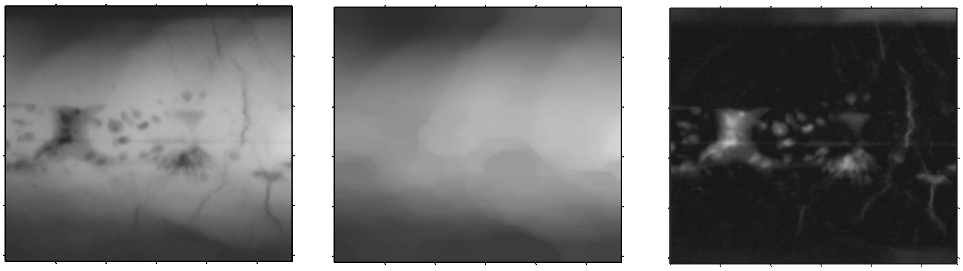

(a) (b) (c)

Figure 3. (a) Original image; (b) Application of the lock operator to the original image; (c) Difference between images (a) and (b).

C) Edge Detection: The purpose of this stage is to determine a separation of the edges of each potential flaw. At this point we define two strategies: edge detection with the Canny filter, and binary thresholding. i) The first strategy uses the method of Canny and the dilation, filling and erosion operations. It is seen that lines have formed around the detected structures (Fig. 4a.), but it is necessary to close them, since the objective consists in generating a set of closed regions from those lines and in that way segment the hypothetical flaws from the image's background. The process continues with the application of the dilation shown in Fig. 4b. The use of this operator allows closing most of the open regions. Then the closed regions from the previous operation are filled; this process is illustrated in Fig. 4c. Finally, the erosion operator is applied to reverse the effect of the dilation and also determine more precisely the zones with flaws from already closed regions.

The method of Canny detects more precisely the edges of the structures because it is less sensitive to noise. Since it uses a Gaussian filter to decrease it; however, it generates a large amount of uncertain edges, and for that reason it is

necessary to carry out the process of dilation, filling and erosion. The disadvantage lies precisely in the generation of open edges, as seen in Fig. 4d; the dotted arrow B indicates a line that has not closed and was detected by the Canny method, but that line does not form a structure that can be closed, even though during the process of dilation and filling it has increased its thickness; the erosion operation returns it to its original state. In another zone of Fig. 4, arrow A indicates the formation of a curve, which suggests the presence of a structure with flaws, however once again the dilation process does not generate a closed region.

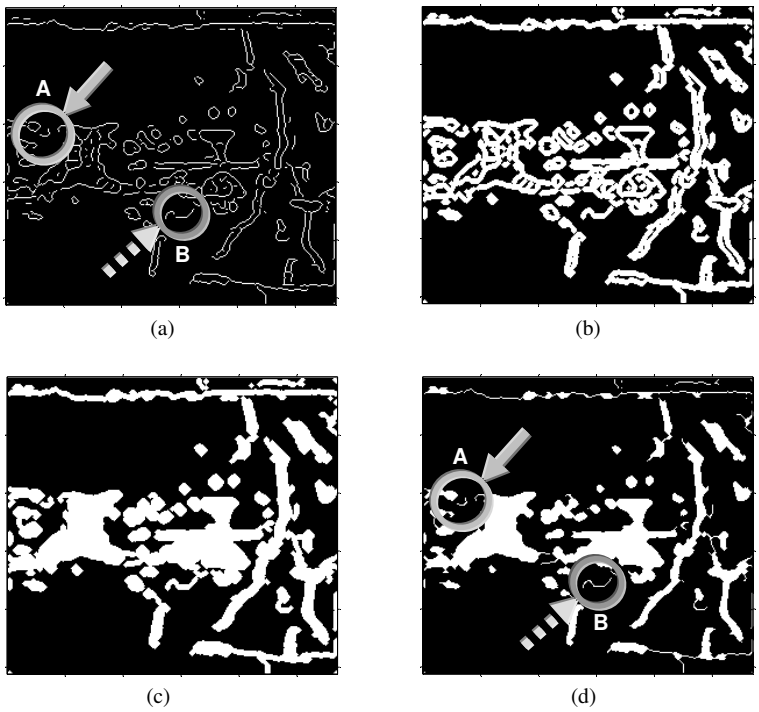

Figure 4. (a) Generation of edges with the method of Canny, (b) Dilation of the edges, (c) Filling of the closed regions, (d) Erosion of the structures.

The binary thresholding strategy consists in applying this operator to the result generated by the bottom-hat filter (Fig. 3c). In this way closed regions are obtained that can be defined by a given threshold. If it is desired to increase the collection of regions, the value of the threshold is decreased so that it allows a greater number of grey levels to pass; conversely, if the threshold is increased, a smaller number of regions are collected. However, the use of this operator generates noise.

The solution consists in applying the opening operator, which results in the generation of an image with low noise level and with uniform and closed structures. The opening operator can be adjusted by changing the size of the structures with which erosion and dilation are applied (Fig. 5b).

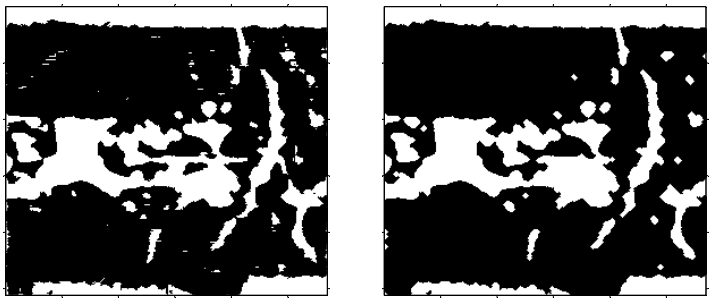

(a) (b)

Figure 5. (a) Binary image produced by thresholding. (b) Application of aperture to image (a).

The main disadvantage compared to the previous strategy is due to the lower detection of edges; the results show that the Canny method generates a large amount of edges in the form of lines without the possibility of closing them. On the other hand, the advantage of binary thresholding consists in generating most of the regions with already closed flaws.

D) Sectioning of original image: Sectioning requires the application of binary thresholding. The idea consists in highlighting and segmenting only those regions with hypothetical flaws. In this point we define two strategies: i) The first consists in rescuing the pixels of the original image from the result of the binary thresholding. The previous result is used as a template that is superimposed on

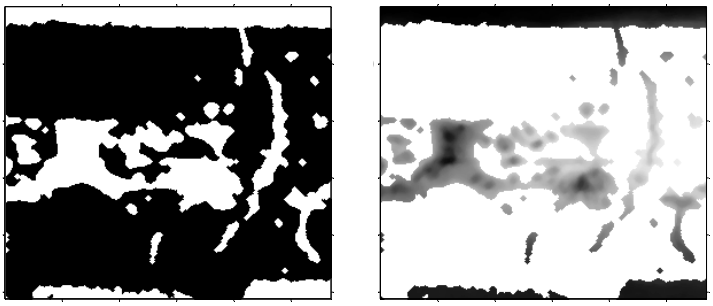

(a) (b)

Figure 6. (a) Binary image from binarization with a given threshold. (b) Copy of pixels of the original image in levels of grey.

the original image (Fig. 6), and in this way it is defined that all the zones or pixels that are black are turned into white, and the white pixels of the binary image are used to copy all the pixels of the original image in the same position. ii) The second strategy uses the distance transform over the white regions, to generate a grey scale surface depending on the distance of its center with respect to its edges (Fig. 7). The purpose is to have a map of the structures with flaws, generated either through the distance transform or as a copy of the original image, because the next process uses the grey levels for segmentation through the watershed transform.

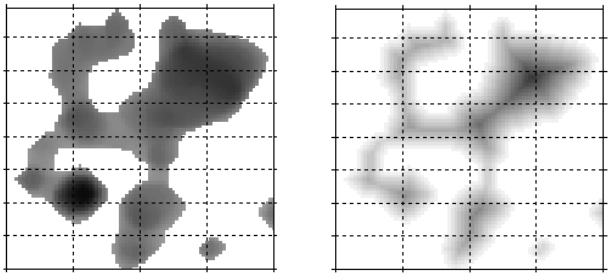

Figure 7. (a) Original pixels from binary mask, (b) Distance transform applied to a binary mask.

When the distance transform is applied to a binary image that has an anthropomorphic shape, undesired results are obtained for later watershed analysis, because the resultant grey scale may not necessarily represent the surface that it is desired to divide. If there are closed circular figures, the differences can be smaller because the resultant formation of the distance operator has the same characteristic as the original image. However, the images that are being studied usually have quite varied shapes and grey scales, and do not represent exact shapes like those mentioned above. From this standpoint the application of the distance transform may not be recommended for the kinds of flaws that are being analyzed, because it does not represent the shape of the grey levels of the original image.

E) Modification of minima: The modification of minima is part of the strategy called “Homotopy modification” [47], which has allowed the avoidance of over segmentation and the generation of more precise segmentation. However, it is important to determine the number of pixels that make up the minimum because a variation in this figure can generate a greater or smaller number of hypothetical flaws (Fig. 8).

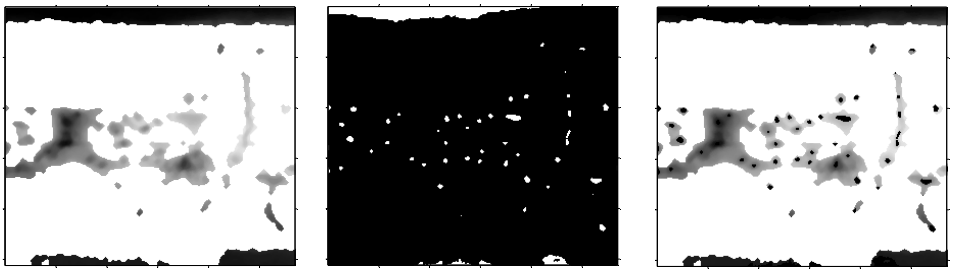

(a) (b) (c)

Figure 8. (a) Binary image. (b) Sections of the binary image on the original image, (c) Calculation of the minimum points of the cut image, (d) Superposition of the minima on image (b).

F) Watershed transformation: The final tool used is the watershed transform. This technique, in combination with the modification of minima, allows the segmentation of structures in the interior of the flaws, because the external segmentation has been carried out previously in the process of binary thresholding. The general segmentation process, especially the binary thresholding stage, has facilitated the generation of the majority of the structures and their edges. It has been shown that the watershed transform by itself does not

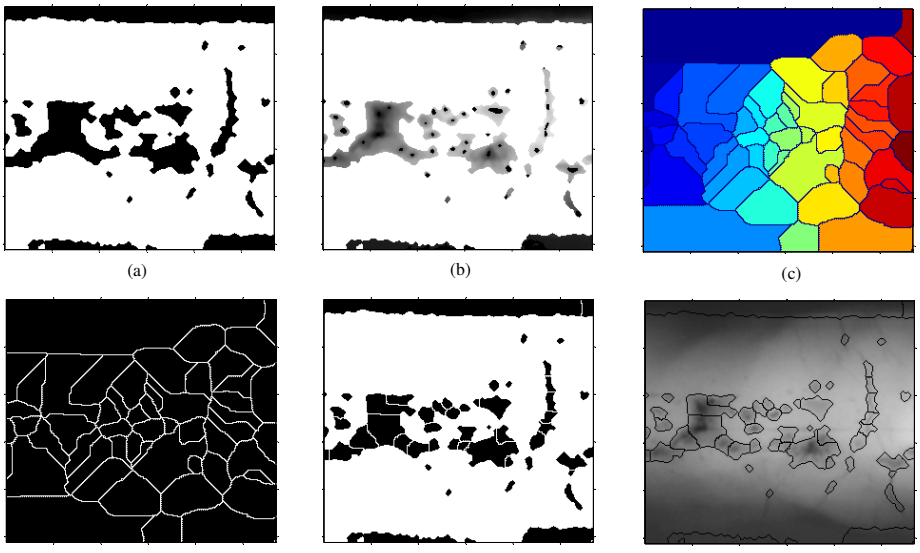

(a) (b) (c)

(d) (e) (f)

Figure 9. (a) Denied binary image. (b) Image with minima superposition. (c) Separation of regions by watershed. (d) Watershed lines. (e) Segmented binary image. (f) Superposition of the cuts on the original image.

generate the segmentation of the defects as it segments the entire image, thus highlighting the importance of the step prior to its application. For that reason, we apply the watershed transform on the structures that can be flawed, because only those regions are segmented and the zones adjacent to the flaws, which have been discarded in the bottom-hat process, are not considered. The whole process is described in Fig. 9.

As the threshold is increased, the segmented regions decrease, and moreover they tend to have a smaller internal area (Fig. 10). Other process variables, such as bottom-hat filter, cut-off point selection, and dilation and erosion operations, influence the number and shape of the regions. However, modifying the variables generates different results, and in some cases this change can lead to imprecise segmentation, and thus it is important to analyze the effect of the modification of each variable, and how it affects the final result (Fig.10).

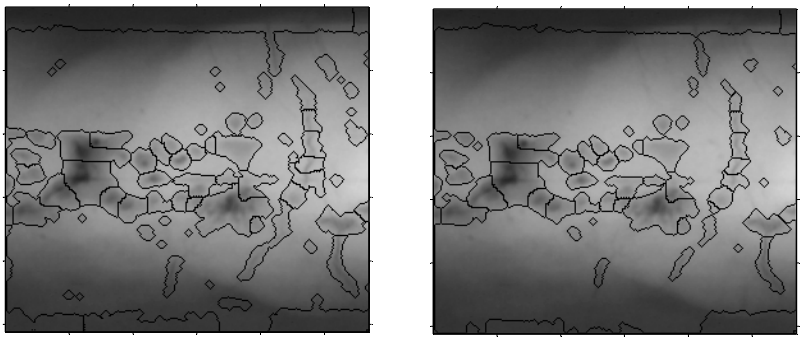

(a) (b)

Figure 10. (a) Segmentation of the image with threshold = 3; (b) Segmentation of the image with threshold = 5.

The resultant segmentation generates an erroneous division not shown in the previous process. For example, if the modification of the minima process is carried out directly on the original image, the result generates a segmentation with respect to the whole image and not on the flawed regions (Fig. 11a). Also, in the case of applying the watershed transform to the original image, without the cuts processing and without the modification of the minima, an over segmentation is generated that does not allow either the determination of the flawed regions or the determination of their location (Fig. 11b).

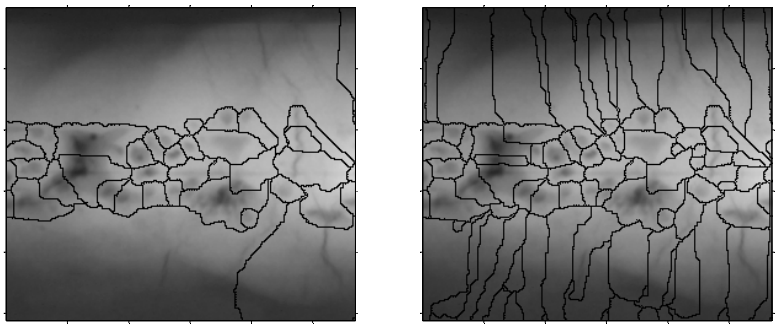

(a) (b)

Figure 11. (a) Watershed segmentation without separation of the regions. (b) Watershed segmentation without the "Homotopy modification" processing.

Summary of the proposed methodology. Every stage of the method proposed in Fig. 2 is respresented in each of the six images of Fig. 12. The image generated at the end of the process with the watershed transform represents the internal and external segmentation of each region.

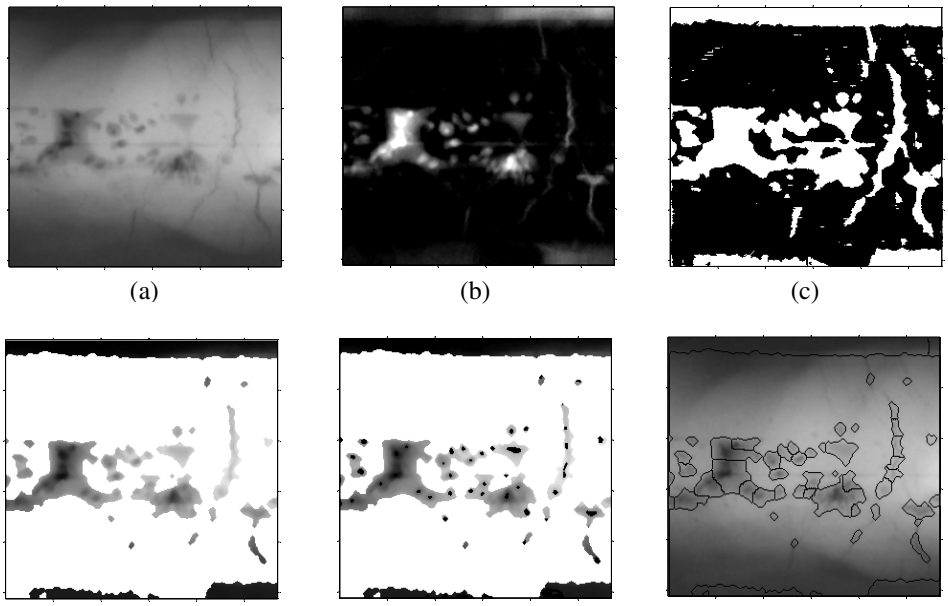

(a) (b) (c)

(d) (e) (f)

Figure 12. Summary of the proposed segmentation process: (a) Image after application of the median filter. (b) Application of the bottom-hat filter. (c) Application of binary thresholding. (d) Application sectioning process. (e) Modification of minima. (f) Application of the watershed transform.

4. Results

The receiver operation characteristic (ROC) analysis is commonly used to measure the performance of a two-class classification. In our case, each feature is analyzed independently using a threshold classifier. In this way a hypothetical flaw is classified as a 'no-defect' (or 'defect') if the value of the feature is below (or above) a threshold value. The ROC curve represents a 'sensitivity' (S_n) versus '1-specificity' ($1\text{-}S_p$), defined as

$$S_n = \frac{TP}{TP+FN} \qquad 1-S_p = \frac{FP}{TN+FP} \tag{1}$$

where TP is the number of true positives (correctly detected defects), TN is the number of true negatives (correctly detected no-defects), FP is the number of false positives (false alarms, or no-defects detected as defects), and FN are false negatives (flaws detected as no-defects). Ideally, $S_n = 1$ and $1\text{-}S_p = 0$, which means that all defects were found without any false alarms. The ROC curve makes it possible to evaluate the performance of the detection process at different points of operation (as defined for example by means of classification thresholds). The area under the curve (A_z) is normally used as a measure of this performance as it indicates how flaw detection can be carried out: a value of $A_z = 1$ indicates an ideal detection, while a value of $A_z = 0.5$ corresponds to random classification [48].

The analysis of the ROC curve is carried out according to the method proposed in [49]. For each image, an ideal detection was achieved using visual interpretation. The methodology was to create an ideal binary image ('1' is defect and '0' is non-defect) according to the visual information with the Microsoft Paint software, using the largest scale (zoom = 800%). The results obtained with our algorithm were then compared with the ideal binary image. Thus, the values for TP, TN, FP and FN were tabulated as shown in Fig. 13.

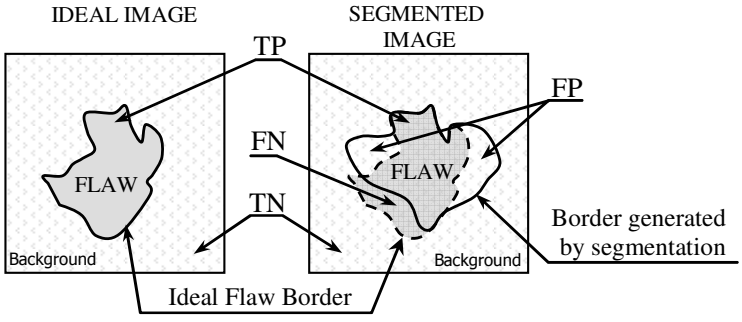

Figure 13. Representation of the differences between the ideal and segmented image.

Table 2. Summary of the segmented images and their best sensitivity and 1-specificity values

Image Name	Number of ideal regions	Regions segmented by the process	Best operational points		A_Z
			Sensitivity	1- Specificity	
BAM5.tif	273	495	90.04%	7.62%	93.08%
12R_M.tif	36	933	96.93%	3.87%	98.03%
13R_M.tif	62	520	90.38%	7.47%	95.22%
22R_M.tif	23	678	94.21%	4.29%	97.44%
28R_M.tif	47	1062	91.08%	5.10%	94.34%
31R_M.tif	11	179	99.51%	0.58%	99.52%
39R_M.tif	90	1110	87.68%	7.86%	94.36%
40R_M.tif	30	731	82.28%	3.74%	91.31%
106R_M.tif	97	836	81.24%	6.17%	89.90%
107R_M.tf	59	2461	80.65%	10.96%	89.41%

Table 2 presents a summary of the images analyzed in this study. The column labelled "Number of ideal regions" presents the number of real regions that must be segmented. The sensitivity and 1-specificity analysis is carried out pixel by pixel using the method proposed in [49]. For this reason, the results differ from those presented in [32], where the regions are analyzed as sets, and not pixel by pixel. The images used correspond to ten of the images catalogued by BAM for non-destructive testing in weld seams. These have been captured using a Lumysis LS85 SDR scanner in high density mode. An LUT linear fit has been used in order to reduce the grey levels of the original images from 12 to 8 bits, and they have been resized to leave only those areas that must be segmented.

In order for the study of the images not to depend on the set analyzed, a generalized ROC curve has been developed. This curve incorporates tests that use the same values with the purpose of obtaining a set of optimum parameters that will allow the use of this filter on an image that is not part of the study. In order to calculate the curve presented in Fig. 14, the values for TP, FN, FP and TN have been added to each test in the study, taking into account that the values being added must be generated on the basis of the same test for each image. Subsequently the 'sensitivity' and '1-specificity' values are calculated.

The ROC curve in Fig. 14 has an area of 93.58%; its best point has an 87.83% sensitivity and a 9.40% 1-specificity. The next-best point has 86.72% sensitivity and a 7.98% 1-specificity. In the latter case the decrease in false alarms is due to the increase in the area of detection, which means that regions with less than 27 pixels are not considered as 'hypothetical flaws.'

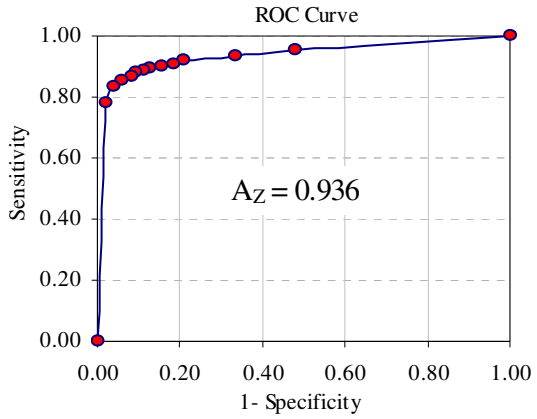

Figure 14. ROC Curve for *TP*, *FN*, *FP*, and *TN* values determined from a set of tests with the same parameters.

The proposed filter has been compared with the method developed in [32]. To carry out the comparison a binary image was been generated manually which contains all the real flaws of the original image. Once the segmented regions have been determined with the use of the proposed filter and the texture analysis filter, the results can be compared against the ideal binary image. As can be seen in Table 3, the results show that the sensitivity for the method developed in this research is 90.94%, compared with 64.13% for the texture analysis method. Moreover, the 1-specificity is 7.62% compared to 4.86% for the texture analysis method. This shows that the proposed method detects a greater number of false alarms, but at the same time detects a greater number of real flaws.

Table 3. Comparison between the developed filter and the texture analysis filter for the BAM-5 image

Image	Process	Segmented regions	Classified regions	Sensitivity	1-Specificity
Bam5.tif	Bottom-hat segmentation (proposed filter)	495	*(na)*	90.04%	7.62%
Bam5.tif	Texture Analysis [32]	1419	187	64.13%	4.86%

The purpose behind having a smaller number of segmented regions is to reduce processing time for the later AVI stages. The type of region being analyzed is important for the process, and consequently the objective must be to decrease the number of segmented regions while simultaneously having a low number of false alarms. To this end the segmentation process must be as precise

as possible in detecting real defects. These results indicate that the proposed filter has two advantages: the first is a reduction in the number of regions, which implies that during subsequent characteristic-extraction and classification processes, fewer regions need to be analyzed, thereby reducing processing time. The second advantage consists in having a high percentage of regions with real flaws and a low percentage of false alarms. This implies that when the segmentation process is applied, the majority of real flaws are included.

5. Conclusions

One of the main filters used in the detection of hypothetical flaws is the bottom-hat filter. Should the flaw have a minimum of contrast with the background, this filter will not detect it. Noise plays an important role in the result of segmentation because if it is too high, a larger mask must be applied, and thus low intensity flaws disappear. On the other hand, if a smaller mask is used, a large number of regions will be generated which will, for the most part, correspond to noise regions.

The analysis of the results indicates that the proposed filter is sensitive to noise: as noise increases, a larger number of regions is detected, and when noise decreases fewer regions are segmented. This effect can be minimized by using a median filter because of its noise attenuating properties and preservation of edge structure.

This work has been compared with the method developed in [32]. The latter method carries out segmentation by means of the LoG filter, extraction is carried out through the co-occurrence matrix and the Gabor function, and finally the classification process is implemented through the use of the polynomial, Mahalanobis and near-neighbor methods. Clearly, comparison with the proposed filter is not entirely fair, as only the segmentation process has been carried out. However, the results may improve on application of the next stages of AVI such as extraction of characteristics and classification. The results indicate that the sensitivity of the proposed method is 90.94%, compared to 64.13% for the texture analysis method. Also, 1-specificity is 7.62% compared to 4.86%, respectively.

Acknowledgments

The authors wish to thank the Federal Institute for Materials Research and Testing, Berlin (BAM) for the radiographic material used in this research. This work was supported in part by Fondecyt Project Number 1040210.

References

[1] E. R. Davis, *Machine Vision*, Third ed. Amsterdam: Morgan Kaufmann Publishers, 2005.

[2] T. S. Newman and A. K. Jain, "A survey of Automated Visual Inspection," *Computer Vision and Image Understanding,* vol. 61, pp. 231-262, 1995.

[3] G. Mamic and M. Bennamoun, "Automatic flaw detection in textiles using a Neyman-Pearson detector," in *Proc. of the international Conference on Pattern Recognition (ICPR)*, Washington, DC, 2000.

[4] L. W. Zhang, A. Dehghani, Z. W. Su, T. King, B. Greenwood, and M. Levesley, "Real-time Automated visual inspection system for contaminant removal from wool," *Real-Time Imaging,* vol. 11, pp. 257-269, 2005.

[5] T. W. Liao, "Classification of welding flaw types with fuzzy expert systems," *Expert Systems with Applications,* vol. 25, pp. 101-111, 2003.

[6] M. Carrasco and D. Mery, "Segmentation of welding discontinuities using a robust algorithm," *Materials Evaluation,* vol. 62, pp. 1142-1147, 2004.

[7] L.-Y. Lei, X.-J. Zhou, and M.-W. Pan, "Automated Vision Inspection System for the Size Measurement of Workpieces," in *Proceedings of the IEEE Instrumentation and Measurement Technology Conference, IMTC 2005*, Ottawa, Canada, 2005, pp. 872-877.

[8] Y.-K. Chung and K.-H. Kim, "Automated visual inspection system of automobile doors and windows using the adaptive feature extraction," in *Second International Conference on Knowledge-Based Intelligent Electronic Systems, KES 98*, Adelaide, Australia, 1998, pp. 286-293.

[9] D. Mery and D. Filbert, "Automated flaw detection in aluminum castings based on the tracking of potential defects in a radioscopic image sequence," *IEEE Trans. Robotics and Automation,* vol. 18, pp. 890-901, Aug. 21 2002.

[10] M. Carrasco and D. Mery, "Automated Visual Inspection using trifocal analysis in an uncalibrated sequence of images," *Materials Evaluation,* vol. 64, pp. 900-906, September 2006.

[11] V.-D. Nguyen, A. Noble, J. Mundy, J. Janning, and J. Ross, "Exhaustive detection of manufacturing flaws as abnormalities," in *IEEE Computer Society Conference on Computer Vision and Pattern Recognition*, 1998, pp. 945-952.

[12] T. H. Park, H. J. Kim, and N. Kim, "Path Planning of automated optical inspection machines for PCB assembly systems," *International Journal of Control Automation and Systems,* vol. 4, pp. 96-104, 2006.

[13] F. Pedreschi, D. Mery, F. Mendoza, and J. M. Aguilera, "Classification of potato chips using pattern recognition," *Journal of Food Science,* vol. 69, pp. E264-E270, 2004.

[14] D. Mery and O. Medina, "Automated Visual Inspection of Glass Bottles using Adapted Median Filtering," *Lecture Notes in Computer Science (LNCS),* vol. 3212, pp. 818-825, 2004.

[15] F. Shafait, S. M. Imran, and S. Klette-Matzat, "Fault detection and localization in empty water bottles through machine vision," in *IEEE, Emerging Technology Conference (E-Tech)*, San Diego, CA, 2004, pp. 30-34.

[16] E. Linhari and V. Obac, "Methodology for Classification of Images based on the characteristics of a new interpretation of Shannon's Entropy," *Wood Science Technology,* vol. 39, pp. 113-128, April 2005.

[17] C. Hayes, "The ABC's of nondestructive weld examination," *Weld. J. (Miami),* vol. 76, pp. 46–51, 1997.

[18] W. Al-Nuaimy and O. Zahran, "Time-of-flight diffraction from semi-automatic inspection to semi-automatic interpretation," *Insight,* vol. 47, pp. 639-644, October 2005.

[19] G. Edward, *Inspection of welded joints. ASM handbook, welding, brazing and soldering* vol. 6. OH: ASM International, 1993.

[20] E. P. de Moura, M. H. S. Siqueira, R. R. da Silva, J. M. A. Rebello, and L. P. Calôba, "Welding defect pattern recognition in TOFD signals. Part 1. Linear classifiers," *Insight,* vol. 47, pp. 777-782, December 2005.

[21] B. Blakeley, "Digital Radiography," *Insight - Non-Destructive Testing and Condition Monitoring,* vol. 46, pp. 403-406, July 2004.

[22] E. Deprins, "Computed radiography in NDT applications," *Insight - Non-Destructive Testing and Condition Monitoring,* vol. 46, pp. 590-593, October 2004.

[23] M. Kleber F., H. Silverio L., T. Mezzadri C., and L. Valeria R. de A., "An object detection and recognition system for weld bead extraction from digital radiographs," *Computer Vision and Image Understanding,* vol. 102, pp. 238 - 249, June 2006.

[24] R. González and R. E. Woods, *Digital Image Processing*, 2nd ed.: Prentice Hall Inc., 2002.

[25] M. Carrasco, "Segmentation of welding defects using digital image processing techniques (In Spanish)," in *Departamento de Ingeniería Informática*. vol. Master of Informatics Engineering Santiago, Chile: Universidad de Santiago de Chile, 2004.

[26] A. Gayer, A. Saya, and A. Shiloh, "Automatic recognition of welding defects in Real-Time radiography," *NDT International,* vol. 23, pp. 131–136, June 1990.

[27] S. W. Lawson and G. A. Parker, "Intelligent Segmentation Of Industrial Radiographic Images Using Neural Networks," in *Proc. of SPIE Machine Vision Applications And Systems Integration III*, 1994, pp. 245–255.

[28] M. Sofia and D. Redouane, "Shapes recognition system applied to the non destructive testing," i*n Proceedings Of The 8th European Conference On Non-Destructive Testing (Ecndt 2002)*, Barcelona, Spain, 2002.

[29] R. R. Silva, M. H. S. Siqueira, L. P. Calôba, I. C. Da Silva, A. A. De Carvalho, and J. M. A. Rebello, "Contribution To The Development Of A Radiographic Inspection Automated System," in *Proceedings of The 8th European Conference On Non-Destructive Testing (ECNDT 2002)*, Barcelona, Spain, 2002.

[30] T. W. Liao and Y. Li, "An Automated Radiographic NDT System For Weld Inspection," *NDT&E International,* vol. 31, pp. 183-192, 1998.

[31] G. Wang and T. W. Liao, "Automatic identification of different types of welding defects in radiographic images," *NDT&E International, Elsevier Science,* vol. 35, pp. 519-528, 2002.

[32] D. Mery and M. A. Berti, "Automatic detection of welding defects using texture features," *Insight, X-Ray Image Processing,* vol. 45, pp. 676-681, October 2003.

[33] G. Li, G. Wang, and Z. Jiguang, "A Genetic Algorithm on Welding Seam Image Segmentation," in *IEEE Proceedings of the 5th World Congress on Intelligent Control and Automation*, Hangzhou. P.R. China, 2004.

[34] K. S. Simunic and S. Loncaric, "A genetic search-based partial image matching," in *Proceedings ICIPS'98 IEEE international conference on Intelligent Processing Systems*, 1998, pp. 119-122.

[35] N. Otsu, "A Threshold Selection Method from Gray level Histogram," *IEEE Transactions on System, Man and Cybernetics,* vol. 9, pp. 62-67, 1979.

[36] X. Wang and B. S. Wong, "Segmentation of radiographic images using fuzzy c-means algorithm," *Insight,* vol. 47, pp. 631-633, October 2005.

[37] D. L. Donoho, "De-noising by soft-thresholding," *IEEE Transactions on Information Theory,* vol. 41, pp. 613-627, 1995.

[38] S. G. Chang, Y. Bin, and M. Vetterli, "Spatially adaptive wavelet thresholding with context modeling for image denoising," *IEEE Transactions on Image Processing,* vol. 9, pp. 1522-1531, 2000.

[39] W. Pedrycz and J. Waletzky, "Fuzzy clustering with partial supervision," *Systems, Man and Cybernetics, Part B, IEEE Transactions on,* vol. 27, pp. 787-795, 1997.

[40] A. Movafeghi, M. H. Kargarnovin, H. Soltanian-Zadeh, M. Taheri, F. Ghasemi, B. Rokrok, K. Edalati, and N. Rastkhah, "Flaw detection improvement of digitized radiographs by morphological transformations," *Insight,* vol. 47, pp. 625-630, 2005.

[41] T. C. Wang and N. B. Karayiannis, "Detection of microcalcifications in digital mammograms using wavelets, " *IEEE Transactions on Medical Imaging,* vol. 17, pp. 498-509, 1998.

[42] K. R. Castleman, *Digital Image Processing*. New Jersey: Prentice-Hall, 1996.

[43] J. Canny, "A Computational Approach To Edge Detection," *IEEE Transactions Pattern Analysis And Machine Intelligence,* vol. 8, pp. 679-698, 1986.

[44] S. Beucher and C. Lantuejoul, "Use of Watersheds in Contour Detection," in *International Workshop on image processing, Real-time edge and Motion detection/estimation*, Rennes, France, 1979, pp. 17-21.

[45] H. Breu, J. Gil, D. Kirkpatrick, and M. Werman, "Linear time Euclidean distance transform algorithms," *IEEE Transactions On Pattern Analysis And Machine Intelligence,* vol. 17, pp. 529-533, May 1995.

[46] L. Vincent, "Morphological grayscale reconstruction in image analysis: applications and efficient algorithms," *Image Processing, IEEE Transactions on,* vol. 2, pp. 176-201, 1993.

[47] S. Beucher, "The Watershed Transformation applied to Image Segmentation," in *10^{th} Pfefferkorn Conf. on Signal and Image Processing in Microscopy and Microanalysis*, 1991, pp. 299-314.

[48] R. O. Duda, P. E. Hart, and D. G. Stork, *Pattern Classification*, Second ed. New York: John Wiley & Sons, Inc., 2001.

[49] D. Mery and F. Pesdreschi, "Segmentation of color food images using a robust algorithm," *Journal of food engineering,* vol. 66, pp. 353-360, 2005.